OPTIMUM DISTANCE BETWEEN VORTEX GENERATORS USED IN MODERN THERMAL SYSTEMS

Azize Akcayoglu, PhD
Cenap Ozgun, M.Sc
Mersin University, Mersin/Turkey
Celal Nazli, M.Sc
Fuat Yilmaz, Ph.D
Gaziantep University, Gaziantep/Turkey
Ali Pinarbasi*, *Ph.D
Yildiz Technical University, Istanbul/Turkey

Abstract

Modern thermal systems in which hydrodynamics and thermal fields are strongly related to each other involve compactness and effective heating/cooling performance. Triangular ducts, having delta-wing type vortex generators (VGs) mounted on the duct's slant surfaces, are widely used in modern thermal systems including gas turbines and electronics cooling applications. Due to the existence of completely opposite results obtained in terms of performance of the two types of VG configurations –namely "flow up" and "flow down"-, in the open literature, in the present study, both hydrodynamics and thermal fields together with the secondary flows induced by the VGs have been analysed extensively to understand which configuration has the better thermo-hydraulic performance. The results show that one configuration has a 19% higher thermo-hydraulic performance over 32 different VG configurations -containing "flow-up" and "flow-down"- for hydraulic diameter based Reynolds number, Re=5000. The angle of inclination of each VG made with the flow direction is set to 30° and the inclined surface's wall temperatures are set to 80°C. Based on the current results, the optimum distance between successive VGs has been determined as 0.385 of the hydraulic diameter. The present CFD results have been validated against the PIV data.

Keywords: PIV (Particle Image Velocimetry), CFD (Computational Fluid Dynamics), vortex generator (VG), thermo-hydraulic performance.

Introduction

As it is well known, hydrodynamics and thermal fields are vitally related to each other in modern thermal systems such as electronics, gas turbines, heat exchangers, aerospace, nuclear and biomedical applications. In these applications, increased efforts have been made to obtain more efficient heat transfer surfaces for non-circular flow passages. Among these passages, triangular ducts are preferred due to their compactness in terms size and volume. As it is stated in (Zhao & Liao, 2002), (Leung & Probert, 1997), (Shah & London, 1978) and (Zhang et al., 2008), maximum convective heat transfer is provided by the equilateral triangular shaped ducts, among other duct shapes, since these ducts can reduce thermal resistance and increase heat transfer coefficient. In addition, when the inner surfaces of the triangular ducts are equipped with the VGs, the heat transfer reached up to 110% (Joardor & Jacobi, 2005) and (Joardor & Jacobi, 2008). The wing-type vortex generators (VG), which have been intensively investigated by Jacobi and Shah (1995) and (Torii, Nishino & Nakayama, 1994), can generate a continuous irregularities on the viscous sub-layer and can increase the heat transfer effectively (Incropera & DeWitt, 1996) and (Biswas, Torii, Fujii & Nishino, 1996). This is achieved by using different VG configurations, namely “flow up” and “flow down”– if the distance between leading edges of the VG pair is more than that of the trailing edges, then the configuration is called “flow up” (Fig. 1a); conversely, if it is less, then it is called “flow down” (Fig. 1b)–(Torii, Kwak & Nishino, 2002) and (Allison & Dally, 2007). Torii et al., Allison and Dally (2007) compared both “flow up” and “flow down” configurations and obtained that “flow up” configuration shows better heat transfer characteristic. However, Kim & Yang (2002), (Fiebig, Valencia & Mitra, 1993) and (Biswas, Mitra & Fiebig, 1994) obtained opposite results. Therefore, the present authors performed extensive studies to find out the best configuration in terms of thermohydraulic performance generated in the equilateral triangular ducts. Thermohydraulic performance is a parameter showing the performance of the modern thermal systems corresponding to maximum heat transfer be obtained by minimum pressure loss to achieve minimum energy consumption (Akcayoglu, Cebeci & Nazli, 2014). In the present investigation, a Computational Fluid Dynamics (CFD) study has been employed to obtain flow and temperature fields in the triangular ducts with 32 different VG configurations. The present simulation results have been validated against the Particle Image Velocimetry (PIV) data of Akcayoglu (2011).

Geometry, Mesh and Numerical Details

The equilateral triangular ducts equipped with VGs studied in this research are shown in Fig. 1a,b,c and d. Each duct is 25.73D long and 1.49D high, where D is the hydraulic diameter of the duct, as shown in Fig. 1. The dimensions, orientations and the locations of VGs are also illustrated in Fig. 1 as Model A, B, C and D. In Fig. 1, b is a varying parameter indicating the distance between successive VGs ($0 \leq b \leq 4.62D$). All the dimensions are selected from the literature Akcayoglu (2011), (Vasudevan, Eswaran & Biswas, 2000) and (Lin, Liu & Leu, 2008) representing the applications in modern thermal systems.

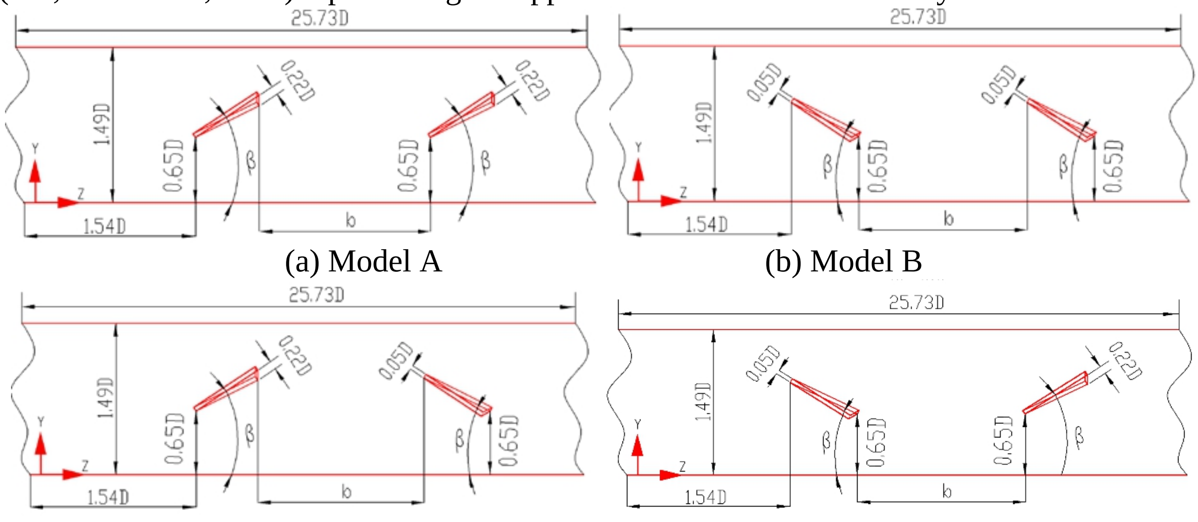

(a) Model A (b) Model B

(c) Model C (d) Model D

Figure 1. Geometrical configurations and locations of VGs.

In the present study, several grid types including different mesh distributions and element sizes are tested and compared with the experimental data to find the best solution. Figure 2 shows four numerical simulation results and an experimental data Akcayoglu (2011) and Akcayoglu et al. (2014) obtained on a line parallel to the x-axis at (y=0.62D, z=4.43D) location. As it is clearly seen from Fig. 2, the results become grid-independent and also are consistent with the experimental data after the element size becomes greater than or equal to 7 million. Therefore, the rest of the simulations are performed using the mesh distribution containing 7 million elements.

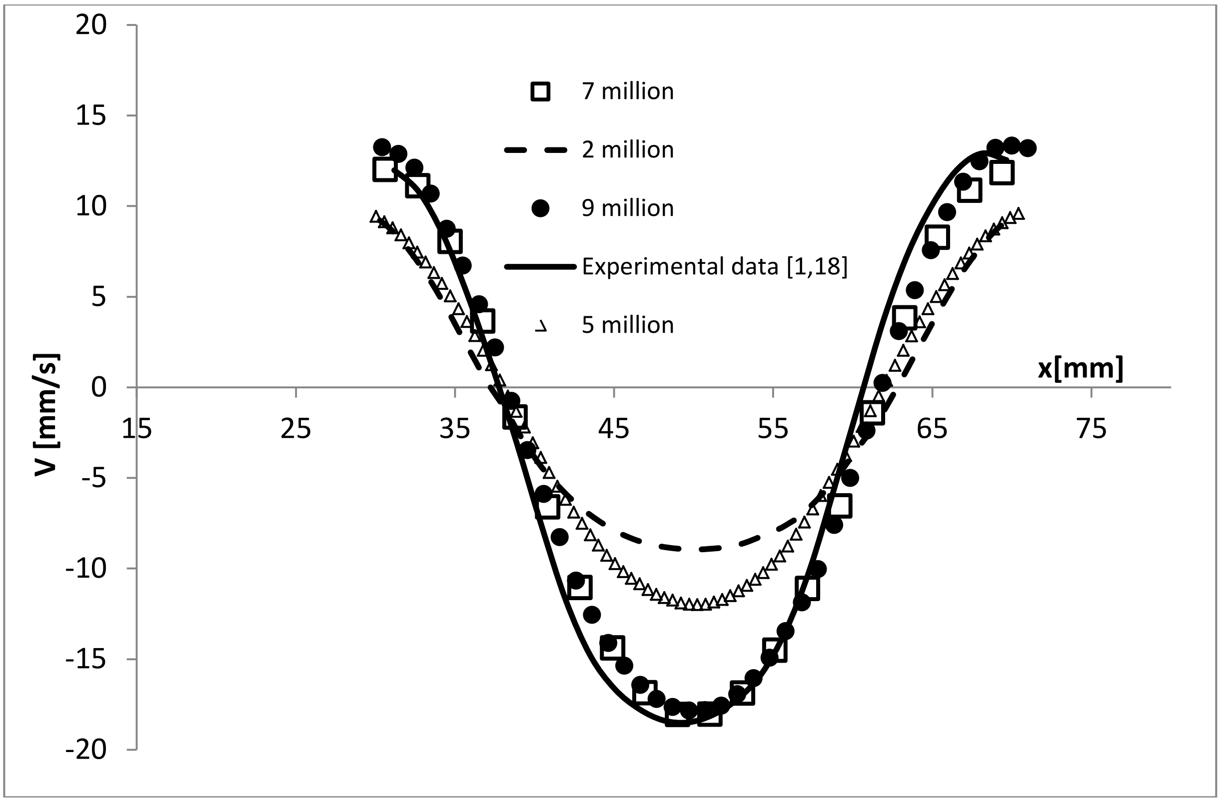

Figure 2. Velocity distribution along x-axis at (y=0.62D, z=4.43D) line [1].

Numerical simulations are carried out by using a finite volume code, ANSYS FLUENT V.14.5. In all simulations, the flow Reynolds number based on the hydraulic diameter of the duct is set to 5000. All fluid properties- including density, viscosity, specific heat and thermal conductivity- are assumed constant. Boundary conditions include “Velocity Inlet” at the duct inlet and “Pressure Outlet” at the duct outlet. A fully-developed velocity profile obtained from experimental results data Akcayoglu (2011) and Akcayoglu et al.(2014) is imposed at the inlet boundary of the domain. The duct base, slant surfaces and VGs are defined as “Wall” boundary condition. The slant surfaces and the VGs are assumed to have constant wall temperature of 80˚C. “Shell conduction” option is enabled in order to compute heat conduction within the walls, to satisfy experimental wall thickness, which is 3 mm data (Akcayoglu, 2011) and (Akcayoglu et al., 2014). In the present study, several turbulence model simulations have been performed for various mesh distributions and the best model has been chosen as “RNG *k-ε*” turbulence model -with “enhanced wall treatment” option- based on the comparison with the experimental data. The continuity, momentum and energy equations are solved to resolve flow and temperature fields within the computational domain. One can refer to ANSYS Inc. (2014) for flow, temperature and model equations. To calculate the thermo-hydraulic performance, the following formulations are used (Webb, Eckert & Golgstein, 1971).

$THP = (Nu / Nu_s) / (f / f_s)^{1/3}$
(1)
$Nu = (hL) / k$
(2)
$h = ((\dot{m}\, c_p (T_{outlet} - T_{inlet})) / (A_{lateral} (T_{surface} - T_{average}))$
(3)
$f = (2\Delta P / (\rho U^2)) (D/L)$
(4)

$\Delta P = P_{inlet} - P_{outlet}$
(5)
$D = 4A_{cross\text{-}sectional} / p$
(6)
$\dot{m} = \rho A_{cross\text{-}sectional} U$
(7)
$T_{average} = ½ (T_{outlet} + T_{inlet})$
(8)

where; f: Friction factor, ΔP: Pressure loss, ρ: Density, U: Mean velocity at the inlet, D: Hydraulic diameter, L: Duct length, p: Perimeter, P_{inlet}: Pressure at inlet, P_{outlet}: Pressure at outlet, h: Heat transfer coefficient, $\dot{m}$: Mass flowrate, c_p: Specific heat capacity, T_{outlet}: Average temperature at outlet, T_{inlet}: Average temperature at inlet, $A_{lateral}$: Total area of lateral surfaces, $T_{surface}$: Average temperature of the heat transfer surfaces, $T_{average}$: Average temperature between inlet and outlet, Nu: Nusselt number, k: Coefficient of thermal conductivity, Nu_s: Nusselt number of smooth duct, f_s: Friction factor of smooth duct, THP: Thermohydraulic performance, $A_{cross\text{-}sectional}$: Cross-sectional area of the duct.

Results

Streamlines are defined as family of curves that are instantaneously tangent to the velocity vector of the flow field studied. When the streamlines are disturbed by the physical structure of the domain, they start to rotate in the flow field, causing the flow velocity to become zero at the center of rotation and this center is called as “focus”. Figure 3 shows streamlines obtained on the xy plane at P=18D for Model D at different VG distances (b), where b is the distance between the successive VGs. Each streamline distributions shown contain 4 foci on the specified plane. As shown in Figs. 3a and 3b, foci pairs formed on the upper part are found smaller compared with the foci formed on the lower part. In addition, all the foci centers shown in Figs. 3a and 3b are found closer to the inclined hot walls of the triangular ducts compared with Figs. 3c and 3d. These results reveal that more heat can be transferred from the hot walls towards the inside of the ducts when the distances between VGs are equal to b=0 and b=0.385D. When b is increased (Figs. 3c and 3d), the upper foci pairs become more dominant while the lower ones getting smaller.

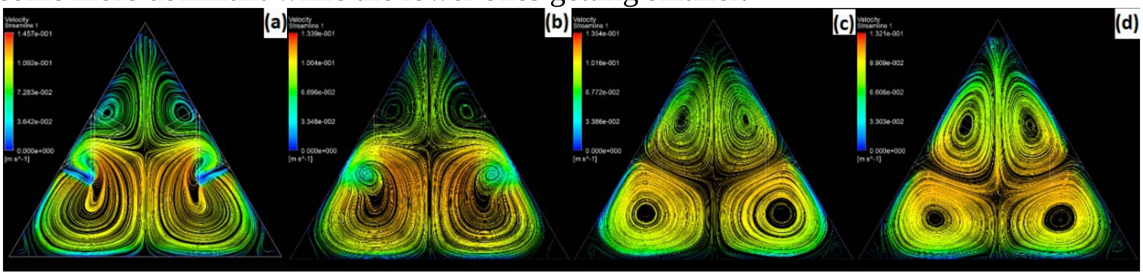

Figure 3. Streamlines obtained on the xy plane at P = 18D for Model D;
(a) b = 0, (b) b = 0.385D, (c) b= 2.31D, (d) b = 4.62D.
(b)

Figure 4 shows streamlines obtained for four different VG configurations for the same successive VG distances, b = 0.385D, on the same plane, P = 18D. It is clear that different streamline distributions are obtained from different VG configurations at P=18D plane. Four foci are observed for Model C and Model D, while only two foci are observed for Model A and Model B (Figs. 4a, 4b, 4c and 4d). In order to find out which configurations have higher THP over the other configurations, it is decided to include temperature distribution obtained on the inclined surfaces of the triangular ducts studied.

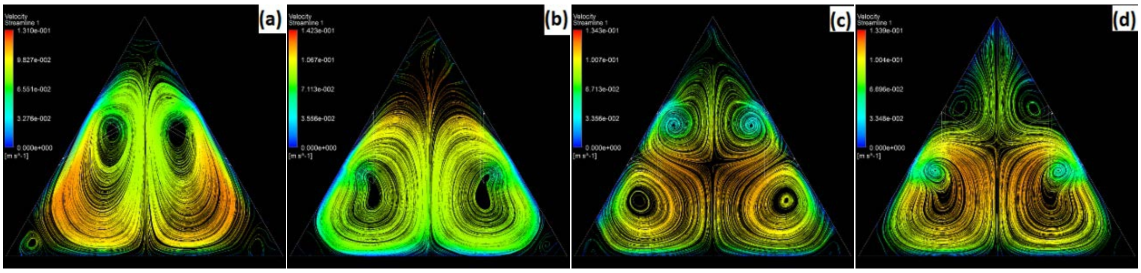

Figure 4. Streamlines obtained for b = 0.385D at P = 18D plane;
(a) Model A, (b) Model B, (c) Model C, (d) Model D.
(b)

Figure 5 shows wall adjacent temperature distributions on the inclined surfaces obtained at different VG distances for Model D. Higher levels of temperature distributions are observed for b=0 and b=0.385D as shown in Figs. 5a and 5b compared with Figs. 5c and 5d. As a result, it is clear that as the distance between the VGs is decreased, then the temperature distributions become better on the inclined walls.

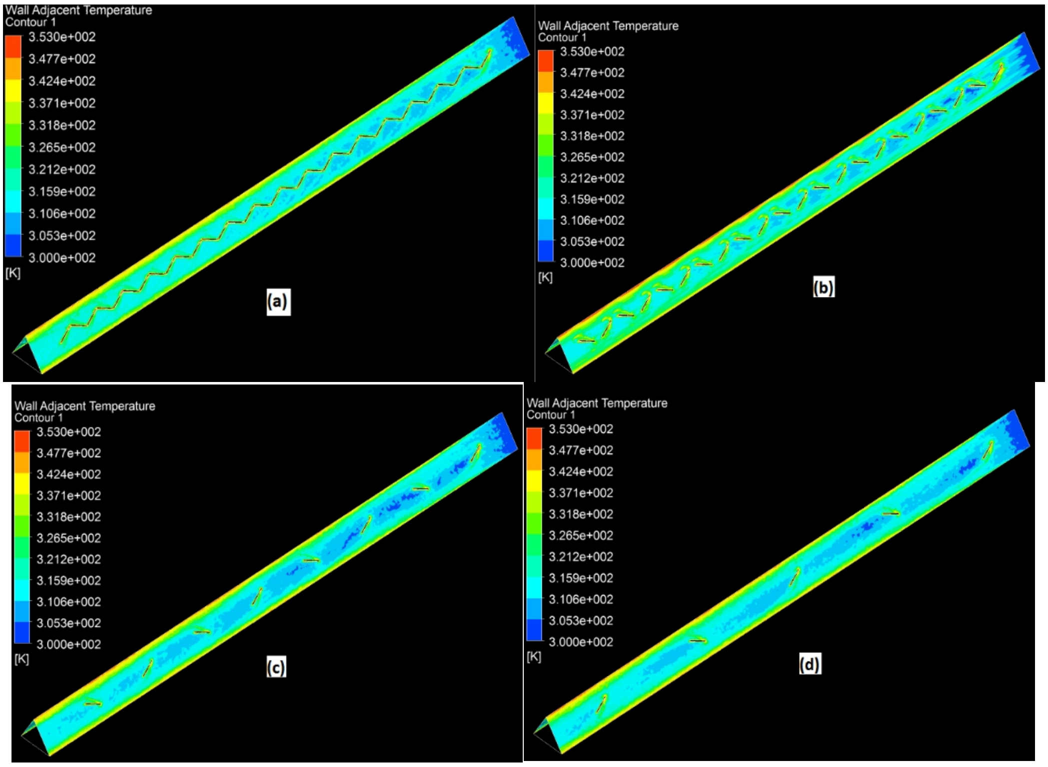

Figure 5. Wall adjacent temperature distribution on the inclined surfaces for Model D;
(a) b = 0, (b) b = 0.385D, (c) b= 2.31D, (d) b = 4.62D.

Wall adjacent temperature contours obtained on the inclined surfaces for each model for b = 0.385D are illustrated in Fig. 6. It is noted that the temperature field is found highly affected by the type of oncoming VG configuration, as higher temperature regions are observed for Model C and Model D, compared with Model A and Model B (Figs. 6a, 6b, 6c and 6d).

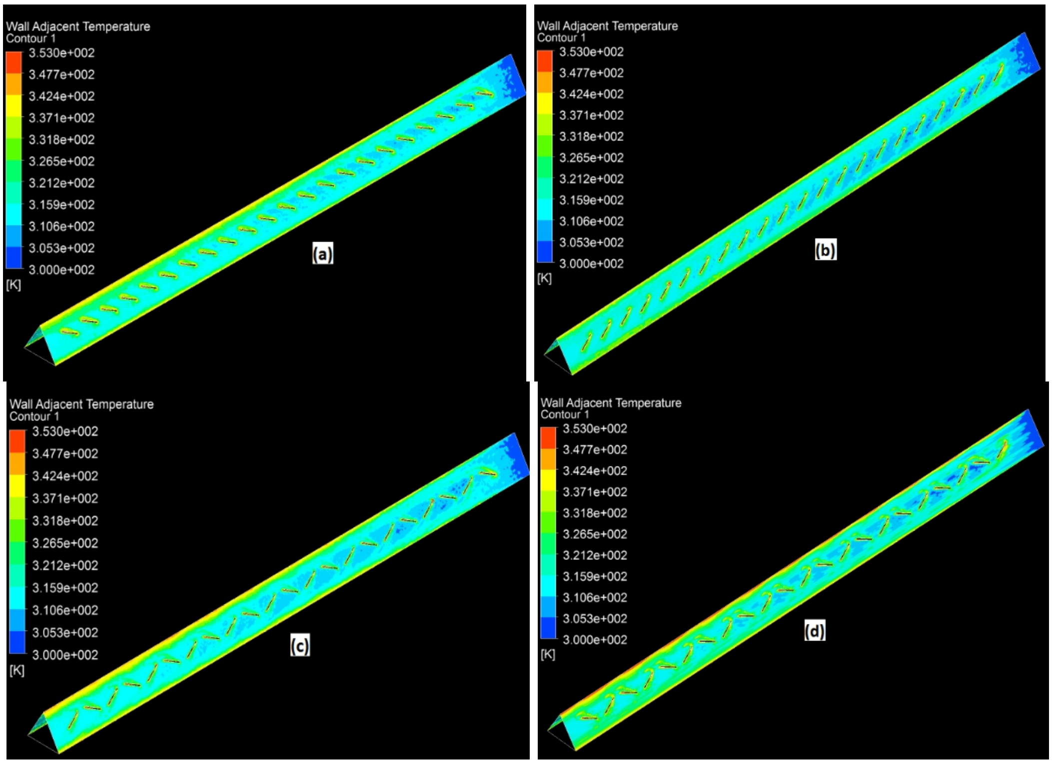

Figure 6. Wall adjacent temperature distribution on the inclined surfaces for b = 0.385D; (a) Model A, (b) Model B, (c) Model C, (d) Model D.

It is known that in modern thermal systems, friction factor f is used as a measure for the pumping power requirement of the system and the Nusselt number is used for the determination of heat transfer of the thermal system. Figure 7a illustrates dimensionless friction factor against distance between successive VGs, b. It is clearly seen that the friction factor decreases when b is increased (Fig 7a). Figure 7b shows dimensionless Nusselt number distribution against distance between successive VGs. The highest Nu is obtained for Model B (Fig. 7b).The smallest values of f and Nu are obtained for Model A, as shown in Fig. 7a and 7b.

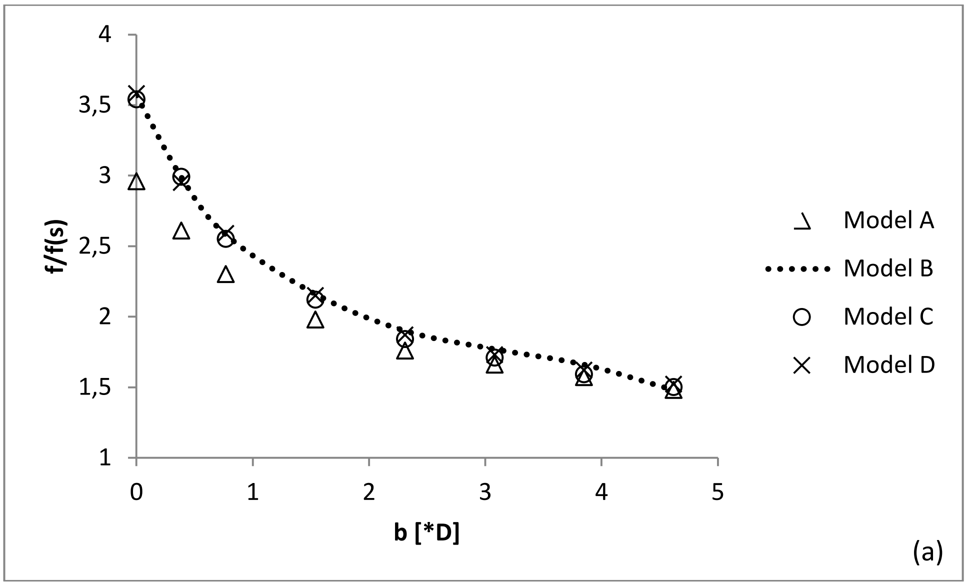

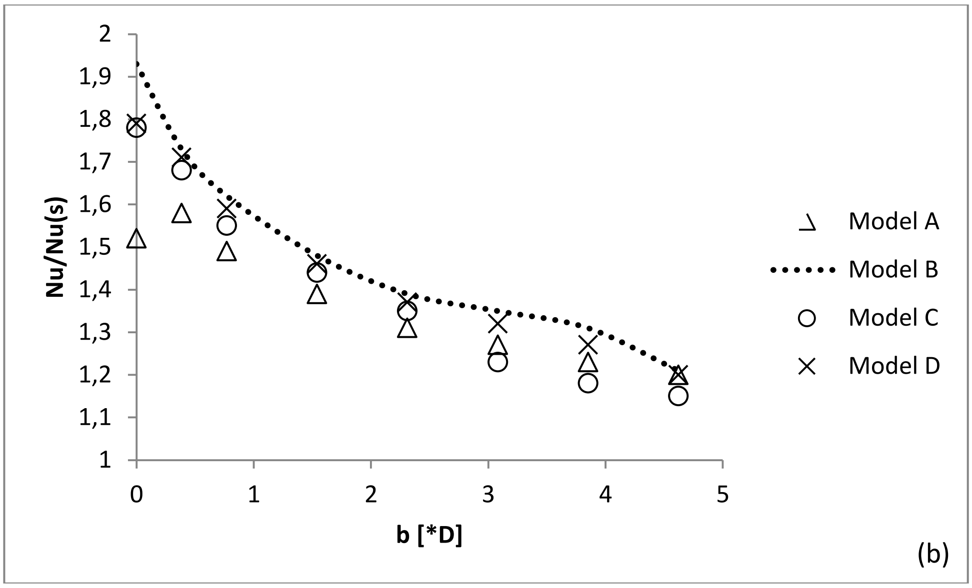

Figure 7. (a) Dimensionless friction factor against distance between successive VGs, (b) Dimensionless Nusselt number against distance between successive VGs.

In order to decide the best VG configuration amongst the cases studied, the thermohdraulic performance (THP) against b is obtained for 32 configurations and the results are illustrated in Fig. 8. As it is seen in Fig. 8, the maximum THP is obtained for Model B. However, THP continuously decreases as b is increased, without showing a peak, for Model B. On the other hand, each of the Models A, C and D have a peak at b = 0.385 D. The maximum peak is obtained for Model D for b = 0.385 D as shown in Fig. 8.

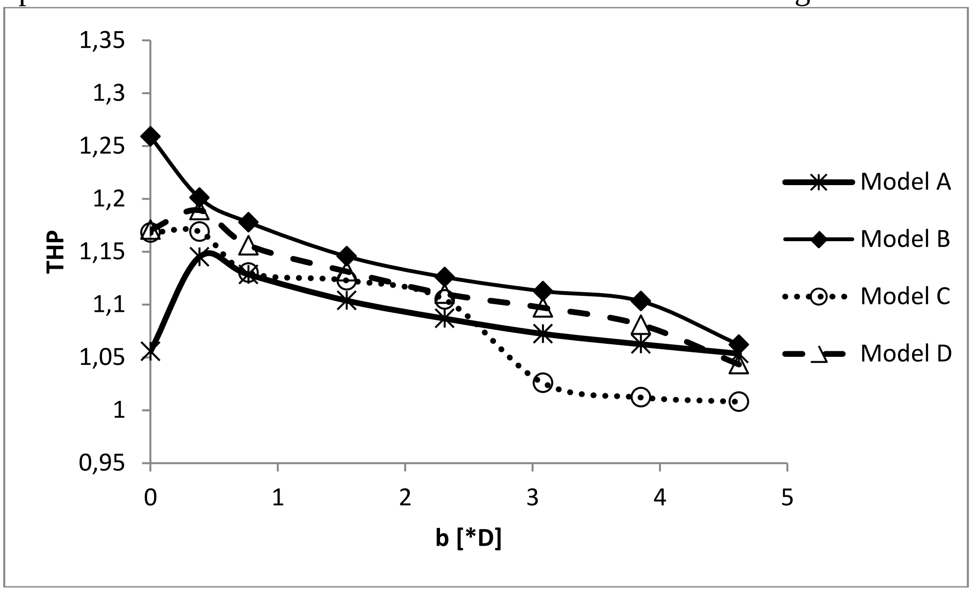

Figure 8. Thermo-hydraulic performance (THP) against distance between successive VGs.

Conclusion

The present numerical study aimed to investigate the best thermohydraulic performance of VG configurations used in modern thermal systems for Re=5000. Both flow and thermal fields are observed carefully and the results are presented for $0 \leq b \leq 4.62D$ where b is the distance between successive VGs. Present results show that the flow and thermal fields are greatly affected by the orientation of VGs as well as the distance between the successive VGs. Higher temperatures are obtained as the distance between the VGs becomes small and as successive VGs are oriented differently- for example if the VG is oriented as “flow down”, then the oncoming VG should be “flow up”. Moreover, comparing to the upper foci pairs, if lower pairs of foci becomes greater, then the THP becomes greater. Among 32 different VG configurations tested, the maximum THP is obtained for b = 0.385D for Model D and is increased 19% in comparison with smooth duct.

Acknowledgement

The present work has been funded by TUBITAK under contract No: 111M726 and has been performed in Mersin University.

References:

Akcayoglu, A., Cebeci, H., Nazli, C. (2014). Thermo-hydraulic performance evaluation of inclined vortex generators, *Advanced Materials Research, 853*, 317-322.
doi:10.4028/www.scientific.net/AMR.853.317

Jacobi, A.M., Shah, R.K. (1995). Heat transfer surface enhancement through the use of longitudinal vortices a review of recent, *Experimental Thermal and Fluid Science, 11*, 295-309.

Torii, K., Nishino, K., Nakayama, K. (1994). Mechanism of heat transfer augmentation by longitudinal vortices in a flat plate boundary layer, *Proceedings of the 10th international heat transfer conference*, 123-128.

Joardor, A., Jacobi, A.M. (2008). Heat transfer enhancement by winglet-type vortex generator arrays in compact plain-fin-and-tube heat exchangers, *International Journal of Refrigeration, 31*, 87-97
doi:10.1016/j.ijrefrig.2007.04.011

Zhao, T.S., Liao, Q. (2002). Theoretical analysis of film condensation heat transfer inside vertical mini triangular channels, *International Journal of Heat and Mass Transfer, 45*, 2829-2842.

Leung, C.W., Probert, S.D. (1997). Forced-convective turbulent flows through horizontal ducts with isosceles-triangular internal cross-sections, *Applying Energy, 57*(1), 13-24.

Shah, R.K., London, A.L. (1978). Laminar flow forced convection in ducts, *New York: Academic Press*, 685, 1978.

Zhang, Y.H., Wu, X., Wang, L.B., Song, K.W., Dong, Y.X., Liu, S. (2008). Comparison of heat transfer performance of tube bank fin with mounted vortex generators to tube bank fin with punched vortex generators, *Experimental Thermal Fluid Science*, *33*(1), 58-66.
doi:10.1016/j.expthermflusci.2008.07.002

Joardor, A., Jacobi, A.M. (2005). Impact of leading edge delta-wing vortex generators on the thermal performance of a flat tube, louvered-fin compact heat exchanger, *International Journal of Heat and Mass Transfer, 48*, 1480-1493.
doi:10.1016/j.ijheatmasstransfer.2004.10.018

Incropera, F.P., DeWitt, D.P. (1996) Introduction to Heat Transfer, *USA: John Wiley & Sons*, 586.

Biswas, G., Torii, K., Fujii, D., Nishino, K. (1996) Numerical and experimental determination of flow structure and heat transfer effects of longitudinal vortices in a channel flow, *International Journal of Heat and Mass Transfer,* 39(16), 3441–3451.

Torii, K., Kwak, K.M., Nishino, K. (2002). Heat transfer enhancement accompanying pressure-loss reduction with winglet-type vortex generators for fin-tube heat exchangers, *International Journal of Heat and Mass Transfer, 45*(18), 3795–3801.

Allison, C.B., Dally, B.B. (2007). Effect of a delta-winglet vortex pair on the performance of a tube-fin heat exchanger, *International Journal of Heat and Mass Transfer, 50*, 5065–5072.
doi:10.1016/j.ijheatmasstransfer.2007.08.003

Kim, E., Yang, J.S. (2002). An experimental study of heat transfer characteristics of a pair of longitudinal vortices using color capturing technique, *International Journal of Heat and Mass Transfer*, *45*, 3349–3356.

Fiebig, M.,Valencia, A., Mitra, N.K. (1993). Wing-type vortex generators for fin-and tube heat exchangers, *Experimental Thermal and Fluid Science, 7*(4), 287-295.

Biswas, G., Mitra, N., Fiebig, K. M. (1994). Heat transfer enhancement in fin-tube heat exchangers by winglet type vortex generators, *International Journal of Heat and Mass Transfer, 37*(2), 283–291.

Webb, R.L., Eckert, E.R.G., Goldstein, R.J. (1971). Heat Transfer and Friction in Tubes with Repeated Rib Roughness, *International Journal of Heat and Mass Transfer, 14*, 601–617.

Akcayoglu, A. (2011). Flow past confined delta-wing type vortex generators, *Experimental Thermal and Fluid Science, 35*, 112-120.
doi:10.1016/j.expthermflusci.2010.08.012

Vasudevan, R., Eswaran, V., Biswas G. (2000). Winglet-type vortex generators for plate fin heat exchangers using triangular fins, *Numerical Heat Transfer*, *58*, 533-555.

Lin, C.N., Liu, Y.W., Leu J.S. (2008). Heat transfer and fluid flow analysis for plate-fin and oval tube heat exchangers with vortex generators, *Heat Transfer Engineering, 29*, 588-596.
doi: 10.1080/01457630801922279

ANSYS Inc. (2014), Documentation. Retrieved from
http://www.ansys.com/Support/Documentation